Newly Developed Stepwise Electroless Deposition Enables a Remarkably Facile Synthesis of Highly Active and Stable Amorphous Pd Nanoparticle Electrocatalysts for Oxygen Reduction Reaction

Kee Chun Poon,[†,‡] Desmond C. L. Tan,[†,‡] Thang D.T. Vo,[†,‡] Bahareh Khezri,[§] Haibin Su,[∥] Richard D. Webster,[§] and Hirotaka Sato*,[†,‡]

[†]School of Mechanical & Aerospace Engineering and [∥]School of Materials Science & Engineering, Nanyang Technological University, 50 Nanyang Avenue, Singapore 639798

[§]Division of Chemistry & Biological Chemistry, School of Physical and Mathematical Sciences, Nanyang Technological University, 21 Nanyang Link, Singapore 637371

S *Supporting Information*

ABSTRACT: This paper reports on highly active and stable amorphous Pd nanoparticle electrocatalysts for the oxygen reduction reaction. The amorphous catalysts were synthesized by a remarkably facile and quick electroless deposition process newly developed in this study (process time <5 min). An electrode substrate (glassy carbon, carbon cloth) was sequentially dipped for 10 s into two separate solutions of a reducing agent (sodium hypophosphite (NaH_2PO_2)) and Pd ions to deposit amorphous Pd nanoparticles containing phosphorus (Pd–P). By repeating the deposition cycles, the specific and mass activities of the Pd nanoparticles can be actively tuned. Owing to the nanoscale amorphous nature, the obtained Pd–P nanoparticle electrocatalysts exhibited superior specific and mass activities compared with crystalline Pd nanoparticles synthesized by another reducing agent (N_2H_4) and commercial Pt-loaded carbon (Pt/C) and Pd-loaded carbon (Pd/C). The specific and mass activities of the amorphous Pd–P nanoparticles were over 4.5 times and 2.6 times higher than previously reported values of Pd and Pt catalysts.

The oxygen reduction reaction (ORR) has attracted much interest because of its importance in the cathodic reaction in fuel cells.[1] This interest, particularly with respect to alkaline fuel cells, has resurfaced because of recent advances in alkaline anion-exchange membranes.[2] Currently, platinum (Pt) electrocatalysts are the best and most widely used catalyst for the ORR. However, due to the high cost of Pt, cheaper alternatives such as Pt-based alloys and non-Pt metals have been researched.[3–15] Pd has emerged as a strong candidate for replacing Pt owing to its significantly lower cost and high catalytic activity.[16–19]

Recent studies on Pd as an electrocatalyst have shown many interesting advancements such as the ability to manipulate the size[16] and shape[20] of Pd nanoparticles, the combination of Pd with other metals to give bimetallic catalysts,[21,22] and the use of various support materials to improve the catalytic activity of Pd.[3,5,6,9,10,16–19] However, very few have studied Pd nanoparticle morphology tuning to improve the catalytic activity, although various other amorphous particles and films exhibit electrocatalytic activity.[23–27]

In this study, stable amorphous Pd nanoparticles were synthesized by stepwise electroless deposition directly onto an electrode. Unlike other processes that require harsh conditions such as high temperature, pressure and long synthesis durations, this process only requires ambient conditions and a remarkably short time for the synthesis process.[16,17,19–21] Such a direct deposition method also does not require additives affecting the catalytic activity,[28–30] thereby significantly improving the ORR. Amorphous Pd nanoparticles synthesized by this process have higher catalytic and mass activities than crystalline Pd nanoparticles and commercial Pt/C and Pd/C for the ORR in KOH (0.1 M) solution. This paper also suggests that the catalytic activity improvement is due to the amorphous phase of the Pd nanoparticles. Moreover, such a high catalytic activity is maintained for long-term, confirmed by a durability test compared with the crystalline Pd nanoparticles, Pt/C, and Pd/C.

The amorphous Pd nanoparticles were synthesized by a stepwise dipping process. A glassy carbon rotating disc electrode (GC-RDE) (3 mm diameter, Bioanalytical Systems, Inc.) was first dipped into 0.2 M NaH_2PO_2 (reducing agent) for 10 s. The electrode was then air-blow dried to remove excess solution adhered to it. The electrode was then dipped into a 2 mM palladium chloride ($PdCl_2$) solution for 10 s, resulting in the reduction of the Pd ions to Pd metal nanoparticles by utilizing only the reducing agent adsorbed onto the electrode surface (i.e., Pd electroless deposition). These steps can be repeated to tune and optimize the catalytic activity of Pd on the electrode surface as in Figure 2. For comparison, the sequence was replicated by varying the reducing agents used (e.g., hydrazine (N_2H_4) instead of NaH_2PO_2).

The Pd nanoparticles synthesized with NaH_2PO_2 (denoted by Pd–P) were small and sparsely dispersed (Figure 1A). Moreover, the halo electron diffraction pattern indicates that the Pd nanoparticles were amorphous. The EDS spectrum of these Pd nanoparticles showed that they contain 11 at% of phosphorus. The X-ray diffraction profile (Figure S1) of the Pd
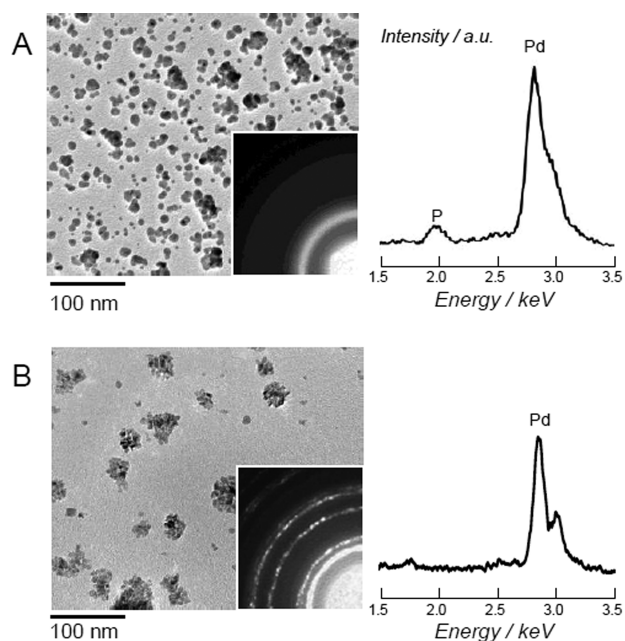
Figure 1. Transmission electron microscopy images, electron diffraction patterns, and energy-dispersive X-ray spectroscopy results from Pd NPs by the stepwise electroless deposition process using reducing agents (A) NaH_2PO_2 and (B) N_2H_4. From the EDS spectra, Pd:P ratio for (A) is 89:11, whereas that for (B) indicates that the particles are pure Pd.

nanoparticles further supports that the Pd nanoparticles were amorphous. On the other hand, Pd nanoparticles synthesized with N_2H_4 (Figure 1B) were also small, but the electron diffraction pattern shows clear Debye−Scherrer rings, proving that the Pd nanoparticles synthesized with N_2H_4 were crystalline.

Linear sweep voltammetry using rotating disk electrodes (RDE) were performed with varying number of deposition cycles to analyze the effect of amorphous Pd−P nanoparticles on the ORR in O_2-saturated KOH (0.1 M) solution compared with that of crystalline Pd nanoparticles, Pt/C, and Pd/C.

Figure 2 shows that the Pd nanoparticles prepared with just three deposition cycles (total synthesis time = 60 s, including 10 s each in the reducing agent and Pd ion solution per cycle) exhibit superior catalytic activity than Pt/C, as indicated by the positive shift in the ORR polarization curve. This trend was observed for Pd nanoparticles synthesized with NaH_2PO_2 (Figure 2A) and N_2H_4 (Figure 2B). The positive shift in the curves increased with the number of deposition cycles.

Notably, a comparison of Pd nanoparticles synthesized with NaH_2PO_2 and N_2H_4 (denoted by Pd−N_2H_4) at the same number of cycles reveals that Pd−P shows superior catalytic activity than Pd−N_2H_4. As summarized in Table 1 from Figure 2, after three cycles, Pd−P exhibited a more positive half-wave potential (0.82 V) than Pd−N_2H_4 (0.78 V) and also an almost similar half-wave potential to that of Pd/C (0.83 V). This increase in catalytic activity of Pd−P nanoparticles was more pronounced at higher number of cycles. In fact, Pd−P at 9 cycles exhibited a more positive half-wave potential (0.85 V) than Pd−N_2H_4 (0.83 V) at 9 cycles or even 18 cycles (0.82 V). The most positive half-wave potential was 0.88 V obtained at 18 cycles of Pd−P. Overall, the results prove that Pd−P nanoparticles exhibit superior catalytic activity than Pd−N_2H_4, Pd/C, and Pt/C.
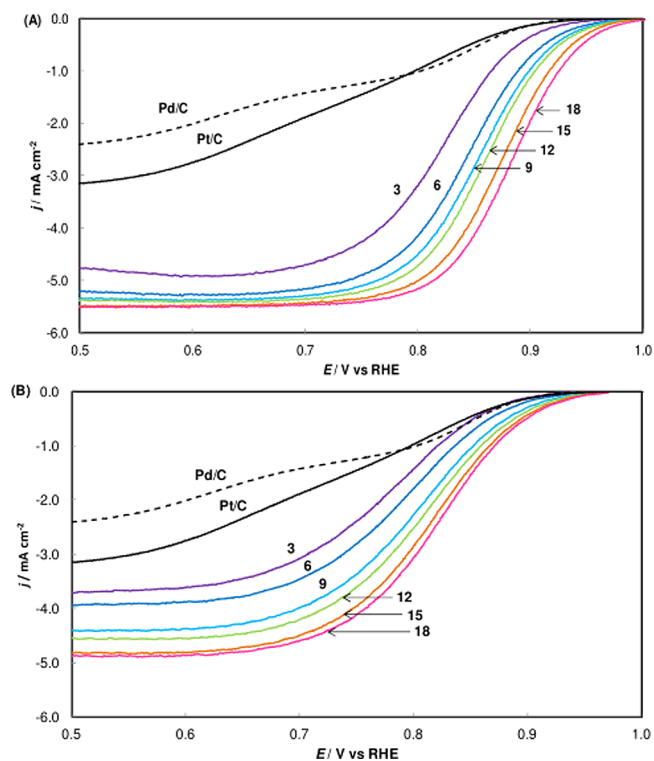
Figure 2. ORR polarization curves for Pd nanoparticles synthesized with (A) NaH_2PO_2 and (B) N_2H_4. The numbers correspond to the cycle numbers of the stepwise electroless deposition process. The measurements were performed in 0.1 M O_2-saturated KOH solution. Scan rate: 10 mV s^{-1}. Rotational speed: 1600 rpm.

Table 1. Half-Wave Potential and Pd (and Pt) Specific and Mass Activity Values[a]

catalyst	half-wave potential (V)	specific activity (mA cm^{-2})	mass activity (mA μg^{-1})
Pt/C	0.74	0.47	0.068
Pd/C	0.83	1.58	0.17
Pd−P (3)	0.82	2.31	1.79
Pd−N_2H_4 (3)	0.78	2.16	1.11
Pd−P (9)	0.85	5.16	2.21
Pd−N_2H_4 (9)	0.83	2.87	1.33
Pd−P (18)	0.88	6.85	1.34
Pd−N_2H_4 (18)	0.82	3.53	1.44

[a]Mass activity and specific activity calculations were according to the method described elsewhere.[19] The values for Pt/C are consistent with that in other papers.[31−35] The values are the average of several numbers of repeated experiments. The current was measured at 0.85 V vs RHE at 1600 rpm. The numbers in the bracket correspond to the cycle numbers of the stepwise electroless deposition process.

From Table 1, Pd−P nanoparticles have the highest active surface among Pt/C, Pd/C, and Pd−N_2H_4 as seen from it having the highest specific activity, which is kinetic current normalized by electrochemically active surface area (ECSA). The maximum specific activity (6.85 mA cm^{-2}) obtained at 18 cycles of Pd−P is over 4.5 times higher than previously reported values of Pd and Pt catalysts.[19] The specific activity is higher at greater number of cycles (9, 18 cycles) than at lower (3 cycles), which suggests initially synthesized Pd−P particles that deposited directly on the glassy carbon surface at lower number of cycles is less active than subsequently synthesized

Pd–P particles that deposited on previously deposited Pd–P particles at greater number of cycles.

The stepwise electroless deposition reasonably saved the Pd loading, resulting in very high mass activity, the kinetic current normalized by mass. Table 1 also shows the mass activity for Pd–P and Pd–N2H4 at different numbers of cycles. The amount of Pd loading was measured by extracting the Pd nanoparticles from the electrode surfaces using concentrated HNO_3 solution and analyzing the samples by inductively coupled plasma-mass spectrometry (ICP-MS). Pt/C followed by Pd/C had the lowest mass activity compared with both Pd–P and Pd–N2H4. Comparing with Pd–N_2H_4, Pd–P is superior at almost all deposition cycle numbers. For 3 cycles, the mass activity of Pd–P (1.79 mA μg^{-1}) was ~1.6 times that of Pd–N_2H_4 (1.11 mA μg^{-1}). This trend was further reflected in samples prepared with 9 cycles (Pd–P 1.6 times greater). For 18 cycles, the mass activity for Pd–P was almost similar to that of Pd–N2H4. To our best knowledge, the mass activity (2.21 mA μg^{-1}) given by 9 cycles Pd–P is the highest value among ever reported electrocatalysts. For instance, it is 2.6 times higher than the one reported in a known paper,[19] while the current density of the Pd–P is higher to that in the paper; thus, the Pd–P synthesized by the stepwise electroless deposition is much more cost-effective as an ORR electrocatalyst.

Figure 3 suggests that the superior catalytic activity is due to the amorphous nature of the Pd–P nanoparticles, as indicated
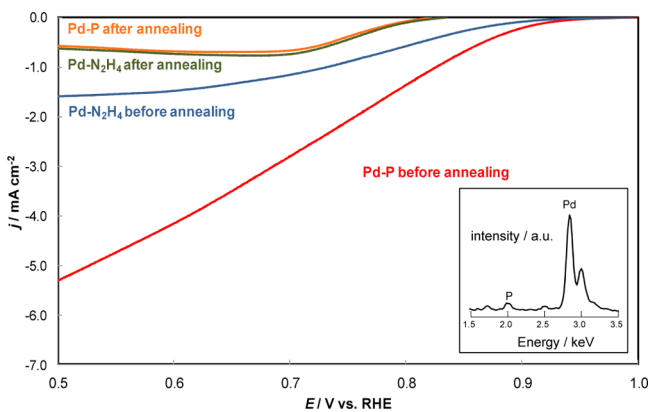
Figure 3. ORR polarization curves of Pd nanoparticles synthesized on carbon cloth. Annealing was performed at 700 °C for 1 h. The measurements were performed in 0.1 M O_2-saturated KOH solution. Scan rate: 10 mV s^{-1}. The inserted figure is the EDS spectra of Pd–P after the annealing, indicating that P remains even after the annealing.

by the polarization curve of the carbon cloth sample annealed at 700 °C for 1 h. Annealing at this temperature and duration changes the amorphous Pd to crystalline phase.[36] After both samples were annealed, the catalytic activity of the Pd–P sample became similar to that of the Pd–N_2H_4 sample (crystalline Pd). Also, phosphorus remained in the Pd nanoparticles even after the annealing, which is confirmed by EDS (Figure 3). Hence, the amorphous nature of Pd–P is the key factor in its superior catalytic activity. The surfaces of Pd–P are more structurally disordered and have more accessible reactive sites with low coordination number in the amorphous nanostructure which may account for the catalytic activity of Pd–P being superior to that of the crystalline Pd–N_2H_4. Such low coordination sites, represented by defects, kinks and edges, are abundant in amorphous structures but not so in crystalline

structures.[37−39] The presence of low-coordination sites has been shown to improve catalytic activity in the ORR.[38−43]

As in Figure 3, the Pd nanoparticles were deposited directly onto carbon cloth. This experiment demonstrates the developed stepwise electroless deposition is suitable for practical preparation of the catalyst sheet for fuel cell. Compared to traditional casting of Pt loaded carbon paste onto carbon cloth,[30] our stepwise electroless deposition is more facile, simpler, and less costly because it deposits catalyst nanoparticles directly onto carbon cloth under ambient condition, and we can actively tune the catalyst load by simply repeating the dipping cycle.

Figure 4, showing the durability test for the ORR of Pd nanoparticles synthesized with NaH_2PO_2 or N_2H_4 and the
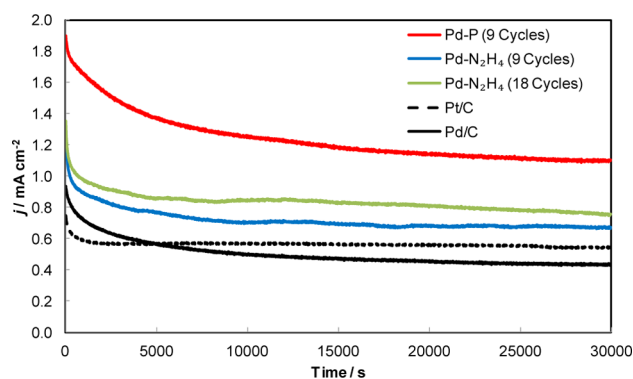
Figure 4. Chronoamperometry response of Pd nanoparticles synthesized with NaH_2PO_2 or N_2H_4. The measurements were performed in 0.1 M O_2-saturated KOH solution, as per the procedure reported elsewhere (potential: 0.666 V vs RHE. Rotational speed: 200 rpm).[1]

commercial Pt/C and Pd/C, demonstrates that the durability of the amorphous Pd–P nanoparticles is enough to keep its catalytic activity being higher than that of Pt/C, Pd/C, and Pd–N_2H_4 nanoparticles prepared with the same number of deposition cycles as well as to that of Pd–N_2H_4 nanoparticles prepared with a greater number of cycles.

In summary, a facile and quick method for synthesizing Pd nanoparticles using NaH_2PO_2 as the preferred reducing agent by stepwise electroless deposition was developed. The specific and mass activities of the obtained Pd nanoparticles containing phosphorus (Pd–P) were higher than any previously reported values. The Pd nanoparticles obtained were amorphous, which may account for their superior specific and mass activities compared with those of crystalline Pd nanoparticles, Pt/C, and Pd/C. Furthermore, the mass activities of these Pd nanoparticles are tunable by varying the number of deposition cycles. The stepwise electroless deposition method was also proven to be effective for practical use with carbon cloth, indicating its suitability for fuel cell industrial applications. The amorphous Pd nanoparticles were durable enough to keep the high catalytic activity for long-term. Overall, these amorphous Pd nanoparticles are a promising alternative to commercial Pd/C and Pt/C for the ORR in alkaline solutions. The stepwise electroless deposition process has the following benefits: (1) Handling is remarkably facile (sequential dipping into two solutions of simple chemical compositions), and reaction time is short (20 s per deposition cycle); (2) catalytic activity is tunable by simply repeating the deposition cycle; (3) no

vacuum, high temperature, or an external power source is needed; and (4) less chemical waste is produced.

In addition, by introducing other metal ion solutions and their mixtures into the process, other pure metals, alloys, or composite nanoparticles can be synthesized. Owing to these benefits, nanoparticles can be widely designed and tailored from theoretical models, not only for ORR electrocatalysis but also for various purposes, and the synthetic process can be automated toward combinatorial chemistry and high-through-put screening.

■ ASSOCIATED CONTENT

Ⓢ Supporting Information

Experimental procedures and XRD patterns of Pd deposits obtained with NaH_2PO_2/N_2H_4. This material is available free of charge via the Internet at http://pubs.acs.org.

■ AUTHOR INFORMATION

Corresponding Author
hirosato@ntu.edu.sg

Author Contributions
‡These authors contributed equally.

Notes
The authors declare no competing financial interest.

■ ACKNOWLEDGMENTS

■ REFERENCES

(1) Guo, S.; Zhang, S.; Wu, L.; Sun, S. *Angew. Chem., Int. Ed.* **2012**, *51*, 11770.

(2) Park, J.-S.; Park, S.-H.; Yim, S.-D.; Yoon, Y.-G.; Lee, W.-Y.; Kim, C.-S. *J. Power Sources* **2008**, *178*, 620.

(3) Chen, Z.; Waje, M.; Li, W.; Yan, Y. *Angew. Chem., Int. Ed.* **2007**, *46*, 4060.

(4) El- Deab, M. S.; Ohsaka, T. *Electrochem. Commun.* **2002**, *4*, 288.

(5) Fernández, J. L.; Walsh, D. A.; Bard, A. J. *J. Am. Chem. Soc.* **2004**, *127*, 357.

(6) Kim, J.; Park, J.-E.; Momma, T.; Osaka, T. *Electrochim. Acta* **2009**, *54*, 3412.

(7) Lin, Y.; Cui, X.; Ye, X. *Electrochem. Commun.* **2005**, *7*, 267.

(8) Matter, P. H.; Zhang, L.; Ozkan, U. S. *J. Catal.* **2006**, *239*, 83.

(9) Shao, M.; Yu, T.; Odell, J. H.; Jin, M.; Xia, Y. *Chem. Commun.* **2011**, *47*, 6566.

(10) Suo, Y.; Zhuang, L.; Lu, J. *Angew. Chem., Int. Ed.* **2007**, *46*, 2862.

(11) Wang, B. *J. Power Sources* **2005**, *152*, 1.

(12) Yan, X.-Y.; Tong, X.-L.; Zhang, Y.-F.; Han, X.-D.; Wang, Y.-Y.; Jin, G.-Q.; Qin, Y.; Guo, X.-Y. *Chem. Commun.* **2012**, *48*, 1892.

(13) Liang, Y.; Li, Y.; Wang, H.; Zhou, J.; Wang, J.; Regier, T.; Dai, H. *Nat. Mater.* **2011**, *10*, 780.

(14) Oezaslan, M.; Hasché, F.; Strasser, P. *J. Electrochem. Soc.* **2012**, *159*, B444.

(15) Tang, Q.; Jiang, L.; Qi, J.; Jiang, Q.; Wang, S.; Sun, G. *Appl. Catal., B* **2011**, *104*, 337.

(16) Jiang, L.; Hsu, A.; Chu, D.; Chen, R. *J. Electrochem. Soc.* **2009**, *156*, B643.

(17) Mentus, S.; Abu Rabi, A.; Jašin, D. *Electrochim. Acta* **2012**, *69*, 174.

(18) Papandrew, A. B.; Chisholm, C. R. I.; Zecevic, S. K.; Veith, G. M.; Zawodzinski, T. A. *J. Electrochem. Soc.* **2013**, *160*, F175.

(19) Seo, M. H.; Choi, S. M.; Kim, H. J.; Kim, W. B. *Electrochem. Commun.* **2011**, *13*, 182.

(20) Erikson, H.; Sarapuu, A.; Alexeyeva, N.; Tammeveski, K.; Solla-Gullón, J.; Feliu, J. M. *Electrochim. Acta* **2012**, *59*, 329.

(21) Maheswari, S.; Sridhar, P.; Pitchumani, S. *Electrochem. Commun.* **2013**, *26*, 97.

(22) Neergat, M.; Gunasekar, V.; Rahul, R. *J. Electroanal. Chem.* **2011**, *658*, 25.

(23) Budniok, A.; Kupka, J. *Electrochim. Acta* **1989**, *34*, 871.

(24) Kreysa, G.; Håkansson, B. *J. Electroanal. Chem. Interfacial Electrochem.* **1986**, *201*, 61.

(25) Podestá, J. J.; Piatti, R. C. V. *Int. J. Hydrogen Energy* **1997**, *22*, 753.

(26) Xiao, L.; Zhuang, L.; Liu, Y.; Lu, J.; Abruña, H. c. D. *J. Am. Chem. Soc.* **2008**, *131*, 602.

(27) Antolini, E. *Energy Environ. Sci.* **2009**, *2*, 915.

(28) Yin, H.; Tang, H.; Wang, D.; Gao, Y.; Tang, Z. *ACS Nano* **2012**, *6*, 8288.

(29) Lee, Y.; Loew, A.; Sun, S. *Chem. Mater.* **2009**, *22*, 755.

(30) Li, D.; Wang, C.; Tripkovic, D.; Sun, S.; Markovic, N. M.; Stamenkovic, V. R. *ACS Catalysis* **2012**, *2*, 1358.

(31) Niu, K.; Yang, B.; Cui, J.; Jin, J.; Fu, X.; Zhao, Q.; Zhang, J. *J. Power Sources* **2013**, *243*, 65.

(32) Yang, W.; Fellinger, T.-P.; Antonietti, M. *J. Am. Chem. Soc.* **2010**, *133*, 206.

(33) Cui, Z.; Burns, R. G.; DiSalvo, F. J. *Chem. Mater.* **2013**, *25*, 3782.

(34) Dong, H.-Q.; Chen, Y.-Y.; Han, M.; Li, S.-L.; Zhang, J.; Li, J.-S.; Lan, Y.-Q.; Dai, Z.-H.; Bao, J.-C. *J. Mater. Chem. A* **2014**, *2*, 1272.

(35) Han, C.; Wang, J.; Gong, Y.; Xu, X.; Li, H.; Wang, Y. *J. Mater. Chem. A* **2014**, *2*, 605.

(36) Gullman, L. O. *J. Less-Common Met.* **1966**, *11*, 157.

(37) Lee, J.-S.; Park, G. S.; Lee, H. I.; Kim, S. T.; Cao, R.; Liu, M.; Cho, J. *Nano Lett.* **2011**, *11*, 5362.

(38) Yang, J.; Xu, J. J. *Electrochem. Commun.* **2003**, *5*, 306.

(39) Lima, F. H. B.; Calegaro, M. L.; Ticianelli, E. A. *J. Electroanal. Chem.* **2006**, *590*, 152.

(40) Cheng, F.; Su, Y.; Liang, J.; Tao, Z.; Chen, J. *Chem. Mater.* **2009**, *22*, 898.

(41) Maciá, M. D.; Campiña, J. M.; Herrero, E.; Feliu, J. M. *J. Electroanal. Chem.* **2004**, *564*, 141.

(42) Kuzume, A.; Herrero, E.; Feliu, J. M. *J. Electroanal. Chem.* **2007**, *599*, 333.

(43) Cheng, F.; Shen, J.; Peng, B.; Pan, Y.; Tao, Z.; Chen, J. *Nat Chem* **2011**, *3*, 79.

(44) Qu, L.; Liu, Y.; Baek, J.-B.; Dai, L. *ACS Nano* **2010**, *4*, 1321.